

# FEDSM2000-11215

## RANDOM FLOW SIMULATIONS WITH A BUBBLE DYNAMICS MODEL

**Andrei Smirnov, Shaoping Shi, Ismail Celik**

West Virginia University

Department of Mechanical and Aerospace Engineering

Morgantown, WV26506-6106

Email:sshi@wvu.edu

### ABSTRACT

In this study we further extend the random flow field generation (RFG) technique of Celik et al. (1999) and also include a Lagrangian particle dynamics routine for efficient particle/bubble tracking in turbulent flows. This algorithm and the mechanism of particle population dynamics can be easily incorporated into general transient flow-field solvers. The random flow-field generation technique enables to generate approximately the random component of the turbulent flow field without actually solving the full Navier Stokes equation. The generated flow-field satisfies the conditions of continuity, anisotropy and inhomogeneity. The random component can then be added to the mean flow-field, obtained as a solution of Reynolds averaged Navier Stokes (RANS) equations or to the velocities of a particulate phase. The former can be used for the generation of initial or inlet conditions in Large Eddy Simulations (LES) while the latter provides an efficient particle tracking technique. The study presents the improved random flow generation procedure (RFG) and demonstrates its feasibility in applications to high-Reynolds number flows in conjunction with the particle tracking algorithm.

### Introduction

Computer simulation of particle dynamics in turbulent flows is usually realized by adding a random component to the particle velocities, which are initially interpolated from a steady-state solution of a Reynolds averaged Navier Stokes (RANS) equations (Zhou and Leschziner,1991; Zhou and Leschziner,1996; Li et al.,1994). RANS modeling produces averaged flow fields, which do not accurately disperse particles that are embedded in

the flow. The Reynolds stress terms are used to generate temporally and spatially correlated fluctuations such that instantaneous velocity fluctuations, which can be superimposed on the particles to induce realistic dispersion. The complexity of the modeling depends on the complexity of the RANS model, which can range from isotropic  $k-\epsilon$  type models up to the anisotropic Reynolds stress (second-moment closure) models. A mechanism for generating a realistic random component of a turbulent flow-field is crucial for the successful application of this technique.

An important relation that any approximation of a random flow-field should satisfy is the relation of mass conservation or continuity. One approach found in the literature (Li et al.,1994) is based on generating an isotropic continuous flow-field proposed earlier by Kraichnan (Kraichnan,1970). However, this flow-field does not satisfy the requirements of spatial inhomogeneity and anisotropy of turbulent shear stresses, which represent other important properties of realistic flows. Another method (Zhou and Leschziner,1991) complies with the latter requirement, but the resultant flow field does not satisfy the continuity condition and is spatially uncorrelated.

In the recent work by Celik at al (1999) the method of Kraichnan was extended to account for the effects of anisotropy and inhomogeneity of turbulence. This allows to simulate a realistic turbulence flow-field, satisfying the continuity, anisotropy and inhomogeneity conditions, at a fraction of a cost of a solution of a full Navier Stokes equation. The technique, which we shall refer to as RFG (Random Flow Generation), enables a more accurate account of turbulence-particle interaction in particulate laden flows and can also be used to generate initial and inflow conditions for Large Eddy Simulations (LES).

In this study we introduce the improved random flow-field generation technique of Celik et al. (1999) and apply it to a Lagrangian particle dynamics routine that was specifically developed for efficient particle/bubble tracking in turbulent flows. The RFG method is further refined and the feasibility of the approach is demonstrated in application to a high Reynolds number ship-wake flow.

## Random flow-field generation method

Particle tracking in transient flows is usually a time-expensive computational procedure. In the situations when the turbulent flow is computed using RANS models it is possible to compute particle dynamics in a steady-state mean flow field and add a fluctuating component to the particle velocities. When LES technique is used the particles should follow a time-dependent flow-field and the fluctuating component should still be added to it at smaller turbulence scales. In both cases the fluctuating component is derived from the turbulence intensity and length-scales, provided by the turbulence model.

In the method of Kraichnan (Kraichnan,1970) a homogeneous isotropic transient flow-field is realized as a superposition of harmonic functions:

$$\begin{aligned} \vec{v}(\vec{x}, t) = & \sqrt{\frac{2}{N}} \sum_{n=1}^N [\vec{v}_1(\vec{k}_n) \cos(\vec{k}_n \cdot \vec{x} + \omega_n t) \\ & + \vec{v}_2(\vec{k}_n) \sin(\vec{k}_n \cdot \vec{x} + \omega_n t)] \\ \vec{v}_1(\vec{k}_n) &= \vec{\zeta}_n \times \vec{k}_n \\ \vec{v}_2(\vec{k}_n) &= \vec{\xi}_n \times \vec{k}_n \\ \vec{k}_n \cdot \vec{v}_1(\vec{k}_n) &= \vec{k}_n \cdot \vec{v}_2(\vec{k}_n) = 0 \end{aligned} \quad (1)$$

where the components of vectors  $\vec{\zeta}_n$  and  $\vec{\xi}_n$  and the frequency  $\omega_n$  are selected from an independent normal distribution with a standard deviation of unity,  $N(0, 1)$ , and the components of wave-numbers  $\vec{k}_n$  are obtained from  $N(0, 1/2)$ . The generated flow-field is homogeneous, isotropic and divergence-free<sup>1</sup>

$$v_{i,i} = 0 \quad (2)$$

$$\overline{v_i v_j} = \delta_{ij} \quad (3)$$

In practical applications increasing the spectral sample size  $N$  will increase the accuracy of reproducing the turbulent spectrum at the cost of longer execution time and higher memory requirements.

<sup>1</sup> $f_{i,j}$  means  $\frac{\partial f}{\partial x_j}$ . Summation is implied for repeated indexes except when index is in parentheses.

Celik et al. (1999) applied a special procedure to  $\vec{v}(\vec{x}, t)$  at each point in space and at every time-step to produce an anisotropic and non-homogeneous flow-field. It involves scaling and orthogonal transformation of  $v_i(\vec{x}, t)$  to produce the new field  $u_i(\vec{x}, t)$  with the pre-defined properties of anisotropy and inhomogeneity. The transformation relations from  $v_i(\vec{x}, t)$  to  $u_i(\vec{x}, t)$  are as follows.

$$v_i^* = v'_{(i)} v_i \quad (4)$$

$$u_i = a_{ik} v_k^* \quad (5)$$

where Eq.(4) provides the scaling and (5) - the orthogonal transformation. Vector  $v'_i$  represents the scale of turbulent fluctuations along  $i$ -th axis. It does not depend on time, whereas vectors  $v_i$  and  $v_i^*$  represent time-dependent velocity fluctuations. The new flow-field  $u_i(\vec{x}, t)$  is transient inhomogeneous and anisotropic with correlation coefficients

$$r_{ij} \equiv \overline{u_i u_j} \quad (6)$$

given as functions of space. Coefficients of orthogonal transformation  $a_{ij}(\vec{x})$  are determined at each spatial location so as to diagonalize  $r_{ij}$

$$r_{ij} = a_{ik} a_{jm} v_{km}^* \quad (7)$$

$$v_{ij}^* = v'_{(i)}^2 \delta_{ij} \quad (8)$$

$$a_{ik} a_{kj} = \delta_{ij} \quad (9)$$

Coefficients  $v'_i$  are determined from Eq.(8) and as the diagonal components of the velocity correlation tensor of  $v_{ij}^* \equiv v_i^* v_j^*$  produced during the diagonalization of  $r_{ij}$  (Eq.7). Eq.(9) is the orthonormality condition on the transformation coefficients  $a_{ij}$ . Thus, the diagonalization procedure applied to the given shear stress tensor  $r_{ij}$  will determine the transformation coefficients  $a_{ij}$  and  $v'_i$ , which are then used in (4) and (5) to simulate the transient field  $u_i(\vec{x}, t)$  with the anisotropy and inhomogeneity properties equal to the pre-defined values  $r_{ij} \equiv \overline{u_i u_j}$ .

Since both  $a_{ij}$  and  $v'_i$  are determined from  $r_{ij}$  they will be functions of space<sup>2</sup>. Because of the averaging operation involved in obtaining  $r_{ij}$  (Eq.6) the length-scale of change of  $r_{ij}(\vec{x})$  is substantially greater than that of the instantaneous velocity  $u_i(\vec{x}, t)$ . In particular, it means that  $|\overline{u_{i,j}|^2} \gg |r_{i,j,k}|$ . Since  $a_{ij}$  are derived from  $r_{ij}$  the same estimate is valid for  $a_{ij}$ , namely

<sup>2</sup>Since  $r_{ij}$  is produced by averaging (Eq.6) it does not depend on time

$|a_{ij,k}| \ll \overline{|u_{i,j}|^2}$ . This in turn means that the divergence-free property of the original flow field  $a_{ij}$  Eq.(2) will be preserved in the orthogonal transformation (5)

$$u_{i,i} \approx a_{ij}a_{ki}v_{j,k} = a_{ji}a_{ik}v_{j,k} = \delta_{jk}v_{j,k} = v_{k,k} = 0 \quad (10)$$

The only other transformation that can affect the continuity condition (2) is the scaling transformation (4). The continuity error can be estimated by differentiating Eq. 4

$$v_{i,i}^*(\vec{x}) = v'_{i,i}(\vec{x})v_i + v'_i(\vec{x})v_{i,i} \quad (11)$$

The first term on the right-hand side represents the effect of inhomogeneity. The second term represents the effect of anisotropy:  $v'_i \neq v'_j$ , ( $i \neq j$ ). When the anisotropy is not negligible the second term constitutes the dominating source of continuity error. This can be shown by the following estimate.

$$\begin{aligned} |v_i| &\sim 1 \\ |v_{i,i}| &\sim 1/l \\ |v'_i| &\sim v' \\ |v'_{i,i}| &\sim v'/L \\ \Rightarrow |v_{i,i}^*| &\sim \frac{v'}{L} + \frac{v'}{l} \approx \frac{v'}{l} \end{aligned} \quad (12)$$

where  $l$  is the turbulence length-scale,  $v'$  is the scale of the turbulent fluctuating velocity, and  $L$  is the length-scale of characteristic variation of  $r_{ij}$ . Since  $L \gg l$  we can neglect the first term in (11) relative to the second one.

The procedure above was tested against experiments in anisotropic and inhomogeneous boundary layer (Hinze,1975; Klebanoff,1954). To compare the simulation results with the experimental data the velocity profile along a vertical line in the center of the axial plane was stored for each simulated realization of the flow-field. The profiles of thousand time realizations were then used to calculate the root mean square fluctuating components in each direction, as well as the corresponding cross correlations. These compare very well with the experimental data as shown in Figure 1.

An improved procedure. The continuity error due to anisotropy (second term in Eq.11) can be eliminated all together by introducing  $v'_i$  as a scaling factor for  $\vec{k}_n$  in (1), i.e.

$$v_i(\vec{x},t) = \sqrt{\frac{2}{N}} \sum_{n=1}^N [v_i^1 \cos(\tilde{k}_j^n x_j + \omega_n t)$$

$$+ v_i^2 \sin(\tilde{k}_j^n x_j + \omega_n t)] \quad (13)$$

$$\tilde{k}_j^n = k_j^n \frac{v'}{v'_{(j)}} \quad (14)$$

where we use the notation  $v_i^1, v_i^2$  for the  $i$ -th components of  $\vec{v}_1, \vec{v}_2$  from Eq.(1). Vectors  $\vec{v}_1, \vec{v}_2, \vec{k}_n$  are generated in the same way as in (1). The flow-field  $v_i$  in (13) is no longer divergence-free. At the same time  $v_i^*$  produced by the scaling transformation (4) satisfies the continuity

$$\begin{aligned} v_{i,i}^* &\approx v'_i v_{i,i} = \\ &= v' \sqrt{\frac{2}{N}} \sum_{n=1}^N [v_i^1 k_i^n \cos(\frac{v'}{v'_j} k_j^n x_j + \omega_n t) \\ &\quad + v_i^2 k_i^n \sin(\frac{v'}{v'_j} k_j^n x_j + \omega_n t)] = 0 \end{aligned} \quad (15)$$

here we neglected all derivatives of  $v'_i$ , which are slowly varying functions of  $\vec{x}$ . The last equality above follows from the orthogonality between  $\vec{v}_1, \vec{v}_2$  and  $\vec{k}_n$ , i.e.  $\vec{v}_1 \cdot \vec{k}_n = \vec{v}_2 \cdot \vec{k}_n = 0$  guaranteed by the way the vectors are constructed in (1).

The performance of the improved procedure was tested by computing the divergence of the generated flow field as a function of turbulence length-scale for three cases: isotropic velocity field (Eq.2), labeled as "Kraichnan", anisotropic velocity field generated according to the algorithm based on Eq.1 (labeled as "Modified Kraichnan"), and anisotropic velocity field generated according to the modified RFG algorithm based on Eq.13 (labeled as "RFG"). For this test case the anisotropy of different fluctuating velocity components was defined by a ratio:  $v'_1 : v'_2 : v'_3 = 0.1 : 1.4 : 1$ . Fig.2 depicts the computed divergence as a function of a ratio of the turbulence length-scale  $l$ , to the grid cell-size.

In all three cases the continuity error decreases with the increase of the turbulence length-scale. This decrease is considerably slower for the anisotropic flow-field generated according to the Eq.1 and is practically the same as for the isotropic flow field. This shows that the generated anisotropic flow field is essentially divergence free. The upper divergence limit for low  $l$  is due to the integration error because of the finite grid size. This limit is set by the estimate of  $\max r_{ij}$ , which is on the order of one.

### Lagrangian particle dynamics

In this work we adopted the particle tracking algorithm of Bocksell and Loth (Bocksell and Loth,1998). This approach is suitable for turbulent flows, which makes it directly applicable to ship-wake flows. The original algorithm was modified for better efficiency by adding a particle population control scheme that

enables seamless particle destruction/creation events without expensive loops over particle arrays. This can be of an advantage in simulations involving a large number of particles.

The position of each particle at time  $t_1$  is computed from the known velocity values using a second order Runge-Kutta time advancing scheme. Spatial dispersion of the bubbles is governed by the turbulent kinetic energy obtained from the turbulence model used to compute the flow field.

To ensure a high accuracy required for LES, the particle dynamics routines need an efficient way of retrieving certain flow quantities, like fluid velocity and turbulent kinetic energy. These values need to be approximated at every particle location. The algorithm that would perform these operations has to be not only accurate enough but also very efficient to enable sufficiently large number of particles in the simulation. For that purpose we wrote a tri-linear interpolation routine formulated for a tetrahedral element. This routine is computationally efficient, it can be applied to both structured and unstructured meshes, and when used for a structured grid of hexahedral elements it approaches second order accuracy on a regular grid.

To realize the above particle dynamics in a fluid flow field given on a grid of velocity vectors separate routines for particle tracking and particle population dynamics were developed. Both routines are optimized for time efficiency by using dynamically linked pointer arrays to avoid expensive loops over grid nodes or searches through the particle set.

## Applications

The particle tracking algorithm was first applied to the flow-field of a bluff body wake.

The LES technique was used to solve the time-dependent, three-dimensional, incompressible Navier-Stokes and scale transport equations in non-orthogonal curvilinear coordinate system (Shi et al.,1999). It is based on a domain decomposition technique, differential sub-grid scale turbulence models and second- and higher order numerical schemes (Zang et al.,1993; Zang et al.,1994).

The bubbles were injected at the two downstream corners of a square prism and convected with the three-dimensional flow-field. The flow data were given on a non-uniform grid of 80x90x20 vertexes at a single point in time. At this stage we considered only the "frozen" flow-field to thoroughly test the interpolation and particle dynamics routines. Figure 3 shows the trajectories of two bubbles injected into this stationary flow. In the frozen flow-field these trajectories represent streak-lines of the flow. Small-scale subgrid turbulence fluctuations should be added to the particle velocities to account for a realistic particle dynamics in a turbulent flow-field.

In the second case the ship-wake flow was considered. A RANS solution to the turbulent ship wake, obtained by the researchers from Rensselaer Polytechnic Institute (Lar-

retéguy,1999) was used. Fig. 4(a) shows the contour lines of a mean velocity field obtained with the RANS ( $k - \epsilon$ ) model. Fig.4(b) shows the snapshot of the non-steady flow field obtained as a superposition of the previous  $k - \epsilon$  solution with the added RFG fluctuating component. The turbulent kinetic energy,  $k$ , and its dissipation rate,  $\epsilon$ , available from the RANS solution were used to set the amplitude and the length-scale of the fluctuating velocity generated by RFG method. As the can be seen from the Fig.4(b) this resulted in a more complicated flow structure in the vicinity of the ship hull.

In the next step we used the particle tracking algorithm for simulation of bubbles in the wake. A simplified equation of bubble motion was used (Elghobashi and Truesdell,1993)

$$\rho_p \frac{dv_i}{dt} = \rho_p f(u_i - v_i)/\tau_p + \rho_f \frac{du_i}{dt} + (\rho_p - \rho_f)g_i + 9.66 \frac{\mu}{\pi d^2} |u_i - v_i| \sqrt{Re_G} \quad (16)$$

where  $d$  is particle diameter,  $\rho_p$  and  $\rho_f$  are particle density and carrier flow density, respectively,  $f$  is the friction coefficient,  $u_i$  and  $v_i$  are carrier flow velocity and particle velocity, respectively,  $g_i$  is the acceleration due to gravity,  $Re_G$  is the shear Reynolds number defined as  $Re_G = \frac{d^2}{v} \frac{du}{dy}$ . The term on the left hand side of (16) is the inertia force, acting on particle due to its acceleration. The terms on the right side are respectively the drag force due to viscosity, fluid pressure gradient and viscous stresses, buoyancy and Saffman lift force (Elghobashi and Truesdell,1993). The Basset force term was neglected, since its contribution can be considered small in highly turbulent flows (Pan and Banerjee,1996) and the added mass term was neglected for brevity in this initial stage of calculations. The integration of Eq.(16), via a second Runge-Kutta scheme provides the new velocity,  $v_i(t)$ , in the  $x_i$  direction for each particle as a function of time.

Figure 5(a) shows the snapshot of a simulation where particles were injected in pulses into the wake flow right behind the ship's stern. At each time step a total of 1000 particles were injected. Although a pulsed injection is not a very realistic mechanism of particle generation, it provides a convenient way of studying the action of a random force by applying it to the initially  $\delta$ -shaped time distribution of particles. The distribution of injection positions was selected with a number density proportional to the level of turbulent kinetic energy at the inlet plane. At every time-step particle velocity was determined by the sum of the mean flow velocity and the fluctuating velocity computed using the RFG technique. In these cases the fluctuating component was added only to the particle velocities to avoid the unnecessary loops over all the grid nodes. It should be noted that this ability to use the RFG procedure only at the prescribed spatial locations offers a definite time-saving advantage in practical computations

and at the same time allows to generate turbulent fluctuations at the subgrid level. The latter qualifies the new RFG technique as a viable subgrid-scale model.

Because of the non-uniform distribution of the turbulent kinetic energy in the ship wake particles experienced especially strong scattering in the pre-axial region of the wake and close to the injection plane. As soon as particles leave the wake region the action of the random forces ceases and particle trajectories align with the mean flow streamlines.

In another simulation (Fig. 5(b)) the bubbles were injected at a single point close to the ship hull where the turbulent kinetic energy was near its maximum. A total of 10 000 particles of 100 microns in diameter were continuously injected into the domain. Two seconds of real-time were simulated for the ship-length of 6m traveling with the speed of 3m/s. The figure shows the tendency of particles to agglomerate in dense groups. The characteristic sizes of these groups are in many instances smaller than the grid-cell size. This reflects the sub-grid nature of the RFG method, which enables it to capture finer details of particle dynamics than can be resolved on an Eulerian grid.

## Conclusions and future work

An improved version of the RFG procedure is developed that enables mass-conservation of a fluctuating velocity-field. The new procedure was tested on the case of anisotropic turbulent flow and showed the satisfaction of continuity with precision limited by the grid resolution.

A particle dynamics algorithm was developed and integrated into the RFG procedure. This algorithm enables efficient computations of particle dynamics in turbulent flow-fields. The procedure was applied to a realistic ship-wake flow.

In the future studies a further grid refinement would be required to resolve smaller structures in LES flow field. A parallel implementation of the algorithm would be appropriate for a sufficient flow field resolution and bubble statistics.

The particle dynamics algorithm should be extended with particle-particle and particle-fluid interaction mechanisms.

Experimental data on bubbles distribution and dynamics in a wake flow would be required to validate the results.

## Acknowledgements

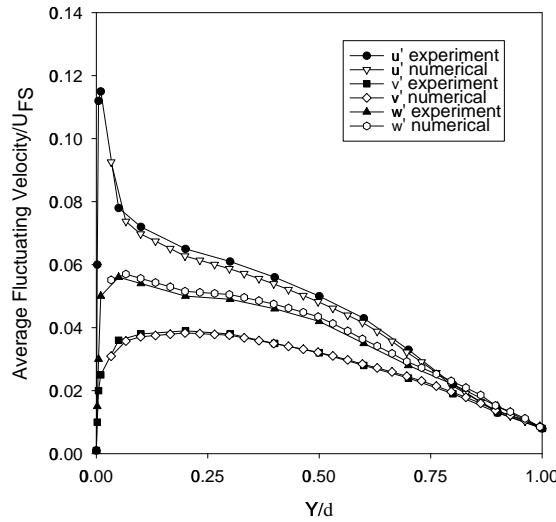
This work has been performed under a DOD EPSCoR project sponsored by the Office of Naval Research (ONR), Grant No. N00014-98-1-0611. The program officer is Dr. Edwin P. Rood.

We thank professor Robert Street of Stanford University, who kindly provided us with the basic LES code. We also thank Dr.Calhoun and Mr.Li Ding in Stanford University for their help with using the code. We thank Dr. Axel Larreteguy of Rensse-

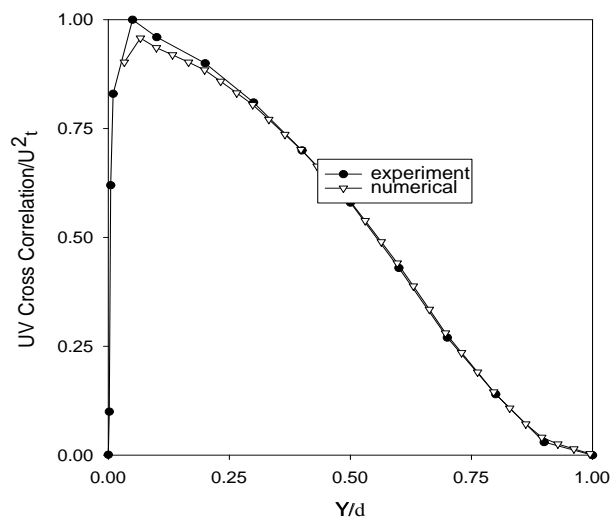
laer Polytechnic Institute for providing the results of the mean flow of a ship model.

## REFERENCES

- Bocksell, T. and Loth, E.: 1998, Random walk models for particle diffusion in wakes and jets, in *ASME Fluids Engineering Division Summer Meeting*, Vol. 5017
- Celik, I., Smirnov, A., and Smith, J.: 1999, Appropriate initial and boundary conditions for LES of a ship wake, in *3rd ASME/JSME Joint Fluids Engineering Conference*, Vol. FEDSM99-7851, San Francisco, California
- Elghobashi, S. and Truesdell, G.: 1993, On the two-way interaction between homogeneous turbulence and dispersed solid particles. i: Turbulence modification, *Physics of Fluids A* **5**, 1790
- Hinze, J.: 1975, *Turbulence, 2nd edition*, McGraw-Hill, New York
- Klebanoff, P.: 1954, *NACA Tech. Notes* 3133
- Kraichnan, R.: 1970, Diffusion by random velocity field, *Phys. Fluid* **11**, 43
- Larreteguy, A.: 1999, *Ship-Wake simulations*, Private communication
- Li, A., Ahmadi, G., Bayer, R., and Gaynes, M.: 1994, Aerosol particle deposition in an obstructed turbulent duct flow, *J. Aerosol Sci.* **25(1)**, 91
- Pan, Y. and Banerjee, S.: 1996, Numerical simulation of particle interactions with wall turbulence, *Phys. Fluids* **8(10)**, 2733
- Shi, S., Celik, I., and Smirnov, A.: 1999, Comparison of different numerical schemes and sub-grid scale models in large-eddy simulation, Boston,Massachusetts
- Zang, Y., Street, R., and Koseff, J.: 1993, A dynamic mixed subgrid-scale model and its application to turbulent recirculating flows, *Phys. Fluids* **5-12**, 3186
- Zang, Y., Street, R., and Koseff, J.: 1994, A non-staggered grid, fractional step method for time-dependent incompressible navier-stokes equations in curvilinear coordinates, *Journal of Computational Physics* **114**, 18
- Zhou, O. and Leschziner, M.: Sept. 1991, A time-correlated stochastic model for particle dispersion in anisotropic turbulence, in *8-th Turbulent Shear Flows Symp.*, Munich
- Zhou, Q. and Leschziner, M.: 1996, *Modelling particle Dispersion in Turbulent Recirculating Flow with an Anisotropy-Resolving Scheme*, Technical Report TFD/96/07, UMIST



(a) Fluctuating velocities



(b) Axial/vertical cross correlations

Figure 1. Comparison with experimental data

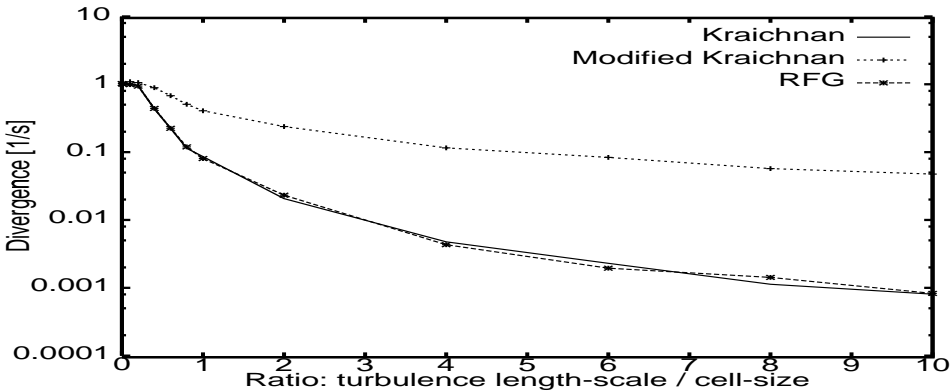


Figure 2. Normalized divergence of an anisotropic velocity field

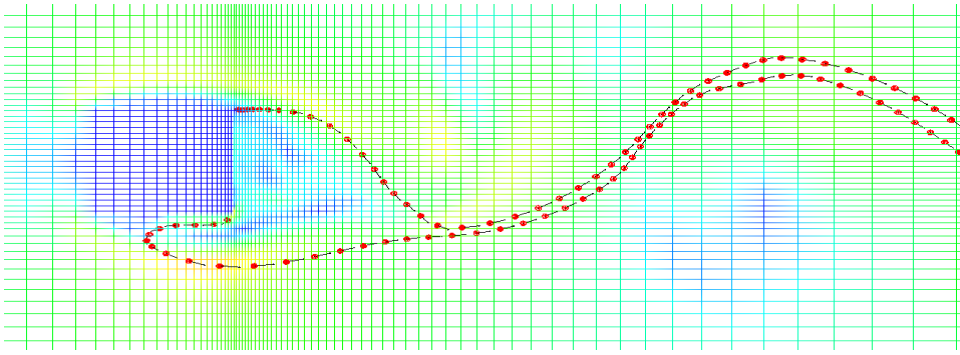
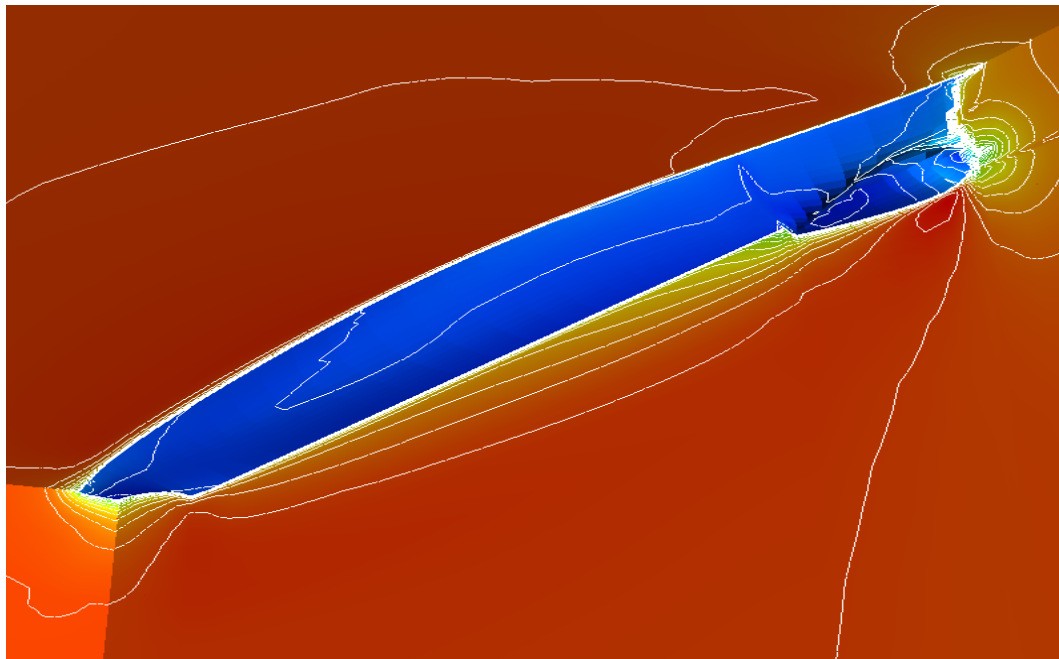
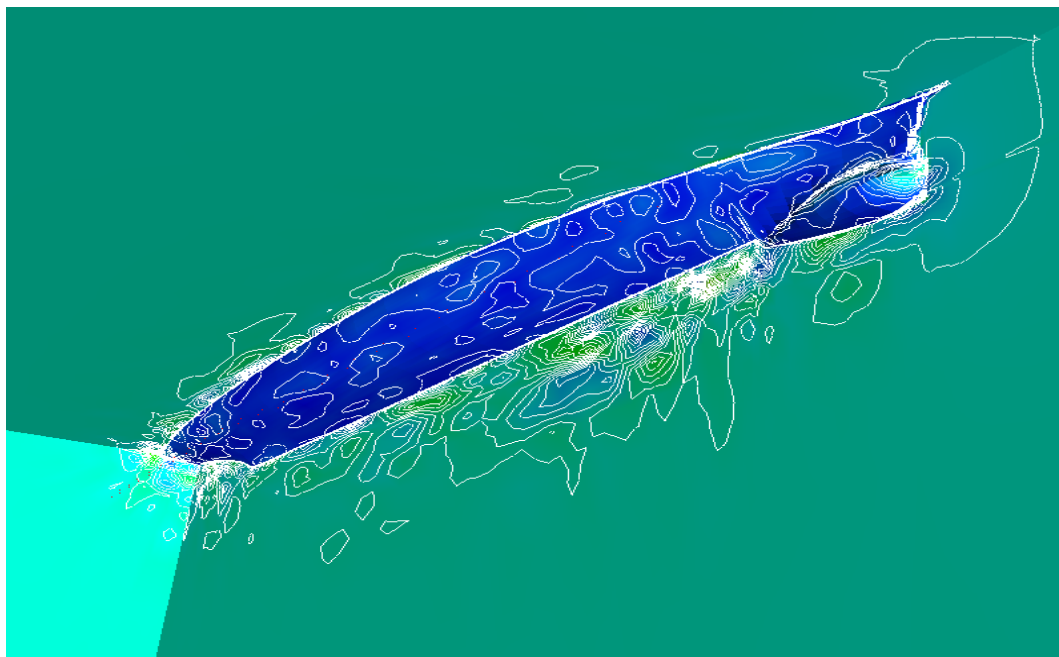


Figure 3. Bubbles in a LES flow of a bluff-body wake



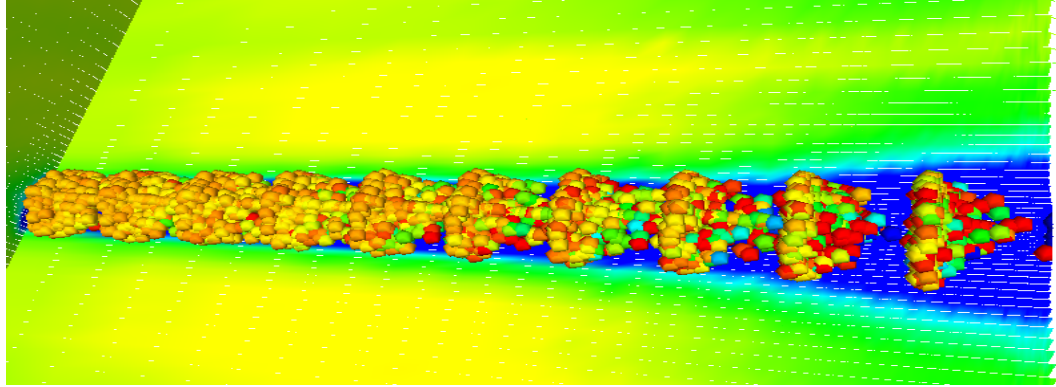
(a) Steady-state RANS calculations



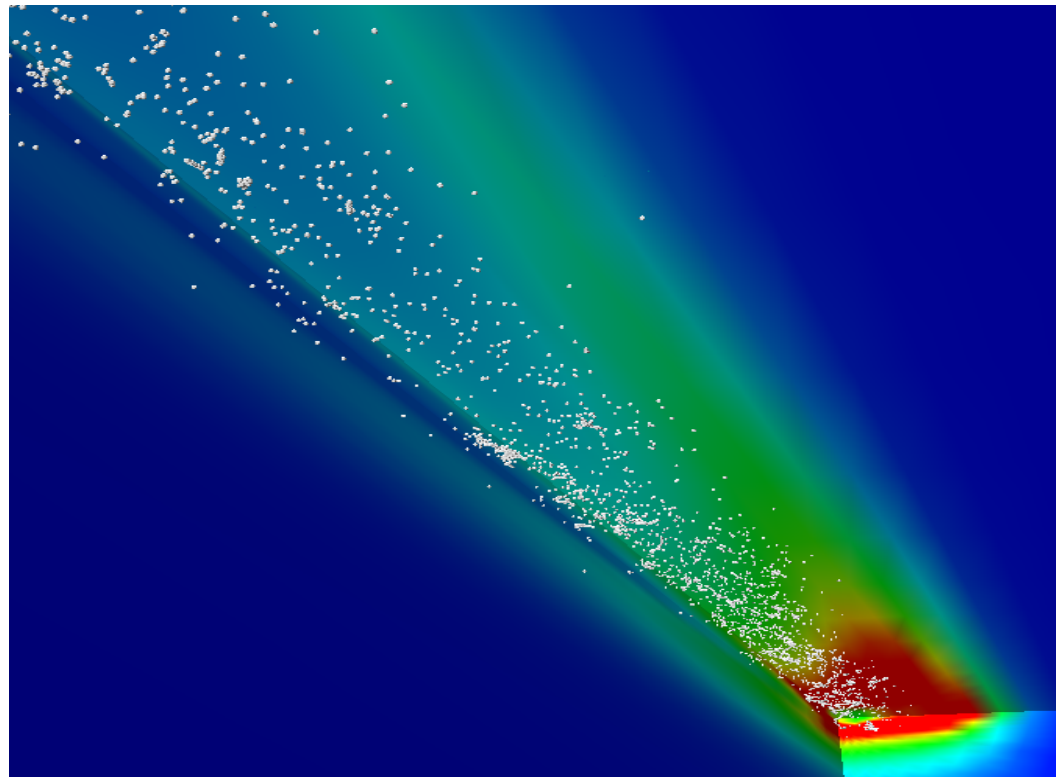
(b) RANS solution with time-dependent fluctuating component

Figure 4. Flow around a ship-hull (view from below)

Contours of velocity magnitude.



(a) 1000 injection points (RANS+RFG solution). Bubble shading is according to velocity magnitude. Direction of flow is from right to left.



(b) A single injection point (10000 bubbles)

Figure 5. Bubbles in a ship wake. Background shading is according to the turbulent kinetic energy.